

# The Evolution of Cluster Early-Type Galaxies over the Past 8 Gyr

Alexander Fritz\*, Inger Jørgensen, Ricardo P. Schiavon, and Kristin Chiboucas

Gemini Observatory, 670 N. A'ohoku Place, Hilo, HI 96720, USA

Received November 23, 2018

**Key words** galaxies: evolution – galaxies: elliptical and lenticular, cD – galaxies: fundamental parameters – galaxies: stellar content – galaxies: clusters: individual (RXJ0152.7-1357, RXJ1226.9+3332, RXJ1415.1+3612)

We present the Fundamental Plane (FP) of early-type galaxies in the clusters of galaxies RXJ1415.1+3612 at  $z = 1.013$ . This is the first detailed FP investigation of cluster early-type galaxies at redshift  $z = 1$ . The distant cluster galaxies follow a steeper FP relation compared to the local FP. The change in the slope of the FP can be interpreted as a mass-dependent evolution. To analyse in more detail the galaxy population in high redshift galaxy clusters at  $0.8 < z < 1$ , we combine our sample with a previous detailed spectroscopic study of 38 early-type galaxies in two distant galaxy clusters, RXJ0152.7-1357 at  $z = 0.83$  and RXJ1226.9+3332 at  $z = 0.89$ . For all clusters Gemini/GMOS spectroscopy with high signal-to-noise and intermediate-resolution has been acquired to measure the internal kinematics and stellar populations of the galaxies. From HST/ACS imaging, surface brightness profiles, morphologies and structural parameters were derived for the galaxy sample. The least massive galaxies ( $M = 2 \times 10^{10} M_{\odot}$ ) in our sample have experienced their most recent major star formation burst at  $z_{\text{form}} \sim 1.1$ . For massive galaxies ( $M > 2 \times 10^{11} M_{\odot}$ ) the bulk of their stellar populations have been formed earlier  $z_{\text{form}} \gtrsim 1.6$ . Our results confirm previous findings by Jørgensen et al. This suggests that the less massive galaxies in the distant clusters have much younger stellar populations than their more massive counterparts. One explanation is that low-mass cluster galaxies have experienced more extended star formation histories with more frequent bursts of star formation with shorter duration compared to the formation history of high-mass cluster galaxies.

© 2009 WILEY-VCH Verlag GmbH & Co. KGaA, Weinheim

## 1 Introduction

Clusters of galaxies at intermediate-redshift ( $1 < z < 2$ ) provide extremely useful laboratories to map the large-scale structure of the universe and study the formation and evolution of cluster galaxies.

There are only a small number of clusters of galaxies known at redshifts  $z > 1$  and our understanding of the galaxy population in these high redshift clusters is limited (e.g., Rosati et al. 2004; Demarco et al. 2007; Lidman et al. 2008; Mei et al. 2009).  $X$ -ray surveys (e.g., Stanford et al. 2001) have detected about a dozen clusters with  $z \geq 1$ . Current surveys carried out in the  $X$ -rays (Romer et al. 2001; Stanford et al. 2006; Finoguenov et al. 2007), optical (e.g., Gladders & Yee 2005), infrared (Stanford et al. 2005; Lawrence et al. 2007), and radio (Branchesi et al. 2006) provide the basis for new but small number of discoveries. Upcoming surveys using the Sunyaev-Zel'dovich effect are expected to discover between 100 to 1000 new massive galaxy clusters at high-redshifts of  $z > 1$  (Carlstrom et al. 2002).

In this context, new spectroscopic observations of clusters of galaxies play a key role for understanding galaxy evolution in dense environments. Previous studies at  $z \sim 1$  concentrated on a few of the brightest (hence more massive  $\gtrsim 2 \times 10^{11} M_{\odot}$ ) early-type cluster members (van Dokkum & Stanford 2003; Holden et al. 2005), because high signal-

to-noise ( $S/N$ ) spectroscopy of distant galaxies is very expensive in telescope time ( $\gtrsim 20$  hours at 8-10m facilities). In particular, these two Fundamental Plane analyses were restricted to three and four brightest early-type cluster members, respectively.

At redshifts of  $z \sim 1.5$ , both cluster (e.g., Cucciati et al. 2006; Cooper et al. 2007) and field (e.g., Bell et al. 2004; Faber et al. 2007; Ferreras et al. 2009; Pozzetti et al. 2009) surveys show a significant increase (by about a factor of two) in the number density of early-type galaxies from higher redshift to the present day. In other words, only about 50% of the total baryonic (stellar) mass in early-type galaxies has been generated before  $z_{\text{form}} \sim 1.5$ , whereas the remainder of the bulk of the stars has been assembled at much later epochs of the universe  $z_{\text{form}} \lesssim 2$ .

Through an investigation of the Fundamental Plane constraints on the evolution and formation history of early-type galaxies as well as their dark matter content are possible. The Fundamental Plane (FP) is a tight linear relation in three-dimensional log-space defined by the effective (half-light) radius  $r_e$ , the average surface brightness within  $r_e$  ( $\langle I_e \rangle$ ) and the central velocity dispersion ( $\sigma$ ) of early-type galaxies (Djorgovski & Davis 1987; Dressler et al. 1987; Jørgensen et al. 1996, hereafter JFK96). This scaling relation has proven to be a powerful tool in measuring the luminosity-weighted average ages of early-type galaxies, both at local (e.g., Bender et al. 1992; JFK96; Bernardi et al. 2003) and at intermediate up to redshifts of  $z \sim 1.2$  (e.g.,

\* Corresponding author: afritz@gemini.edu

Jørgensen et al. 1999; Wuyts et al. 2004; Fritz et al. 2005; di Serego Alighieri et al. 2005; Treu et al. 2005; Jørgensen et al. 2006, 2007; Fritz et al. 2009). The mean age of the stellar populations in these galaxies can be directly probed, because an evolution in the zero-point offset of the FP with increasing redshift can be directly related to a change in the average mass-to-light ( $M/L$ ) ratio of the galaxies under consideration.

At  $z \sim 1$  our understanding of the FP is very limited. Previous works based on small number statistics at  $z \sim 1.3$  found a FP relation with a large intrinsic scatter, twice as high as in the Coma cluster (van Dokkum & Stanford 2003; Holden et al. 2005), with the properties of these early-type cluster galaxies poorly understood. This larger intrinsic scatter is in disagreement with the FP for two galaxy clusters at  $z = 0.8 - 0.9$  (Jørgensen et al. 2006, 2007). In this high redshift domain selection effects play an important role. Therefore, both large, well defined sample sizes as well as high quality data are needed to separate observational limitations (like sample selection or cosmic variance) from the underlying physical processes in these distant galaxies (see also discussion in Fritz et al. 2009).

We present the FP for 12 early-type galaxies at  $z = 1.013$  that are associated with the rich, massive and  $X$ -ray luminous cluster of galaxies RXJ1415.1+3612. The galaxy cluster has been observed using a combination of high  $S/N$  GMOS spectroscopy at the 8m Gemini North telescope and deep imaging of the Advanced Camera for Surveys (ACS) onboard Hubble Space Telescope (HST). Our most distant sample reaches an absolute magnitude limit of  $M_B \sim -21$  mag (rest-frame), which makes this work less susceptible to selection effects. Our study of RXJ1415.1+3612 is part of the Gemini/HST Galaxy Cluster Project (Jørgensen et al. 2005), an extensive observational program to investigate the evolution, star formation and chemical enrichment history of galaxies in rich galaxy clusters from  $z = 1$  to the present-day universe. Previous results on the Gemini/HST Galaxy Cluster Project have been published on the stellar populations of the cluster RXJ0152.7-1357 at  $z = 0.83$  (Jørgensen et al. 2005), the stellar content and FP of RXJ0142.0+2131 at  $z=0.28$  (Barr et al. 2005, 2006) and the FP of RXJ0152.7-1357 and RXJ1226.9+3332 at  $z = 0.89$  (Jørgensen et al. 2006, 2007). Throughout this article we adopt a  $\Lambda$ CDM cosmology for a flat low-density Universe with  $H_0=70 \text{ km s}^{-1} \text{ Mpc}^{-1}$ ,  $\Omega_M = 0.3$ , and  $\Omega_\Lambda = 0.7$ . Unless otherwise noted, all magnitudes are given in the Vega system.

## 2 The Gemini/HST Galaxy Cluster Project

The Gemini/HST Galaxy Cluster Project (PI: I. Jørgensen) is an extensive observational campaign to investigate the formation and evolution of distant galaxies in rich galaxy clusters from  $z = 1$  to the present-day (Jørgensen et al. 2005). For 15 massive,  $X$ -ray luminous selected galaxy clusters from  $z = 0.1$  to 1, optical intermediate-resolution Gemini/GMOS spectroscopy and HST/ACS+WFPC2 ima-

ging have been acquired. These rich galaxy clusters have  $X$ -ray luminosities in the order of  $L_X (0.1 - 2.4 \text{ keV}) = 2 \times 10^{44} \text{ ergs s}^{-1}$ , which in particular range from about 0.5–1 times the  $X$ -ray luminosity of the Coma galaxy cluster. The high  $S/N$  and moderately high resolution ( $\langle S/N \rangle \sim 25 \text{ \AA}^{-1}$  in the rest-frame) in the GMOS galaxy spectra allows us to study in detail the internal kinematics and stellar populations of the galaxies. The nearby Coma, Perseus and Abell 4038 galaxy clusters at  $z = 0.02$  are used as local comparison samples (Jørgensen et al. 1995; 2005; JFK96). The properties and selection effects of this sample have been extensively tested and therefore are well understood (JFK96; Jørgensen 1999).

The main science drivers and objectives of the galaxy cluster project are (see also partly Jørgensen et al. 2005):

- Investigate the star formation history (SFH) of cluster galaxies as a function of redshift;
- Study the early-type galaxy population over a wide mass range at  $z = 1$ ;
- Construct scaling relations and study the evolution of their zero-point, slope and scatter;
- Test the evolution for different galaxy morphologies;
- Measure absorption line strengths to constrain the evolution of the stellar populations and the overall chemistry in the galaxies;
- Constrain the chemical enrichment history of the galaxies by computing ages, metallicities and abundance ratios;
- Test the model predictions for possible variations in the initial mass function (IMF);
- Search for possible dynamical and morphological substructure of the clusters under investigation.

The combined results for all of these approaches will enable a detailed picture of the involved formation processes and subsequent evolution of galaxies over the past 8 Gyr.

## 3 RXJ1415.1+3612: Observations and Data

### 3.1 GMOS Spectroscopy

Target galaxies were selected using colour-colour and colour-magnitude diagrams based on deep ground-based  $r'i'z'$  GMOS-N imaging of the central  $5'.5 \times 5'.5$  field of the rich clusters of galaxies RXJ1415.1+3612 at  $z = 1.013$  down to  $z_{850} < 23.87$  mag (Jørgensen et al. 2009, in prep). Follow-up MOS spectroscopy of 37 galaxies in the field of RXJ1415.1+3612 was acquired with the Gemini Multi-Object Spectrograph (GMOS-N, Hook et al. 2004) at Gemini North in queue mode in dark time in 2005 as part of Gemini program GN-2005A-Q-33. The imaging data for RXJ1415.1+3612 were observed as part of Gemini programs GN-2003A-DD-4 and GN-2003A-SV-80. Spectroscopic observations made use of the unique nod-and-shuffle (N&S) GMOS mode at Gemini (Glazebrook & Bland-Hawthorn 2001) to reach both the magnitude limit and to avoid limitations of sky-subtraction systematics. Briefly, the N&S observing technique allows an improved subtraction of strong

telluric night sky emission lines for faint targets by using telescope (nod) and detector charge shifts (shuffle), while reading out the detector only after 30 minutes of integration. A series of 48 individual exposures yielded a total integration time of 24 hours. Adopting an instrument setup with slit widths of  $1''$  and the R400 grating results in a resolving power of  $R \sim 2000$  and an instrument resolution in the final spectra of  $\sigma \sim 105 \text{ km s}^{-1}$  at  $4300\text{\AA}$ , which is sufficient to measure both internal kinematics (velocity dispersions) and absorption line-strengths of the galaxies. The longpass filter OG515\_G0306 was used to avoid second order contamination of the spectra.

Radial velocities and velocity dispersions ( $\sigma$ ) of the galaxies were measured using a penalized maximum-likelihood fitting algorithm in pixel space (Gebhardt et al. 2003). To ensure a reliable error treatment and test the impact of systematic effects, Jørgensen et al. (2005) performed Monte Carlo simulations for artificially generated galaxy spectra and different stellar templates. Results showed that the  $S/N$  of the galaxy spectra does not significantly affect the systematic error. Galaxies with low velocity dispersions ( $\log \sigma \leq 1.74$ ), which is  $1/2$  times the instrumental resolution might be subjected to systematic effects and therefore have been excluded from the analysis of the scaling relations. The spectroscopy of RXJ1415.1+3612 will be published in Jørgensen et al. (2009).

The GMOS N&S observations for RXJ1415.1+3612 yielded in a total spectroscopic sample of  $N_{\text{spec}} = 37$  galaxies. Out of this sample, 18 galaxies are cluster members, of which 14 galaxies are within the ACS field-of-view of the galaxy cluster. For two galaxies out of these 14 inside the ACS field, no velocity dispersion could be derived due to low  $S/N$  of those spectra.

### 3.2 HST/ACS Photometry

We use deep HST/ACS imaging for RXJ1415.1+3612 from the HST archive which was acquired during Cycle 14 (GO 10496, PI: S. Perlmutter). The primary aim of this program is to search for "dust free" supernovae of Type Ia (SNe Ia) in high-redshift clusters to constrain dark energy time variations. Each of the eight individual pointings in the F850LP filter was split into four exposure times of 340 s to 375 s, yielding a total integration time of 9920 s. The observations in the F775W filter will not be used in the following. The HST/ACS surface brightness distribution of 30 galaxies within the ACS pointing of the galaxy cluster was modelled using the publicly available 2D fitting algorithm GALFIT (Peng et al. 2002). Each galaxy surface brightness profile was separately analysed with seeing-convolved, sky-corrected model profiles. ACS structural parameters (total magnitude, effective (half-light) radius  $r_e$ , and average surface brightness within  $r_e$ ,  $\langle I_e \rangle$ ) were derived by fitting a pure de Vaucouleurs ( $r^{1/4}$ ) profile to the luminosity distribution of the galaxy of interest. Afterwards the derived photometry were calibrated to rest-frame Johnson  $B$ -band

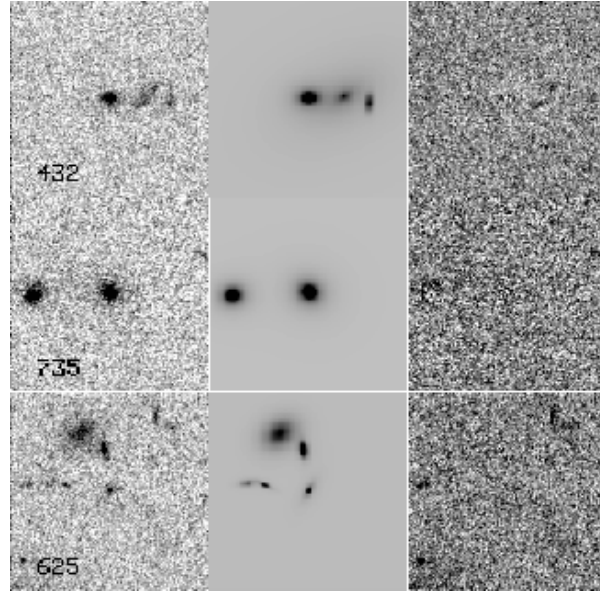


**Fig. 1** HST/ACS surface brightness modelling for three cluster galaxies in RXJ1415.1+3612 at  $z = 1.02$ . The examples show the results of  $r^{1/4}$ -law models for three different cluster members over a wide range in magnitudes and sub-structure. Close neighbouring galaxies were independently modelled and then subtracted. Left panel: Distortion corrected ACS original image, middle panel: Adopted model with neighbouring objects that are subtracted out, Right panel: Residual image.

using our  $r'i'z'$  GMOS photometry and also with evolutionary synthesis models (see Jørgensen et al. 2005 for details). We also tested the effects of other surface brightness models (e.g. single Sersic fits with varying  $n$ -parameter) on the structural parameters. The results remained very stable for our galaxies. In particular, the combination of the FP parameter that enters the FP,  $(\log r_e + \beta \log \langle I_e \rangle)$  with  $\beta$  in the range  $0.7 < \beta < 0.8$ , is highly stable and differs only little for the choice of the profile (Fritz et al. 2005; Chiboucas et al. 2009). Elliptical (E) and S0 galaxies were morphologically classified using a visual inspection, the profile fitting results, and their bulge-to-total fractions. For the following analysis, however, the early-type galaxies are treated as one homogenous group and no separation into the different morphological sub-classes has been made. To account for point-spread function (PSF) variation and distortion effects, a unique PSF was generated for each galaxy according to its position on the ACS chip using the TinyTim version 6.2 package (Krist 1995). Similar results are found when, instead of artificially created PSF stars, real star measurements are used (Chiboucas et al. 2009).

In Fig. 1 we show the distortion corrected ACS image of three different cluster members over a wide range in magnitudes and sub-structure along with the adopted model and residual images. Close neighbouring galaxies were independently modelled and then subtracted. Fig. 1 gives the results

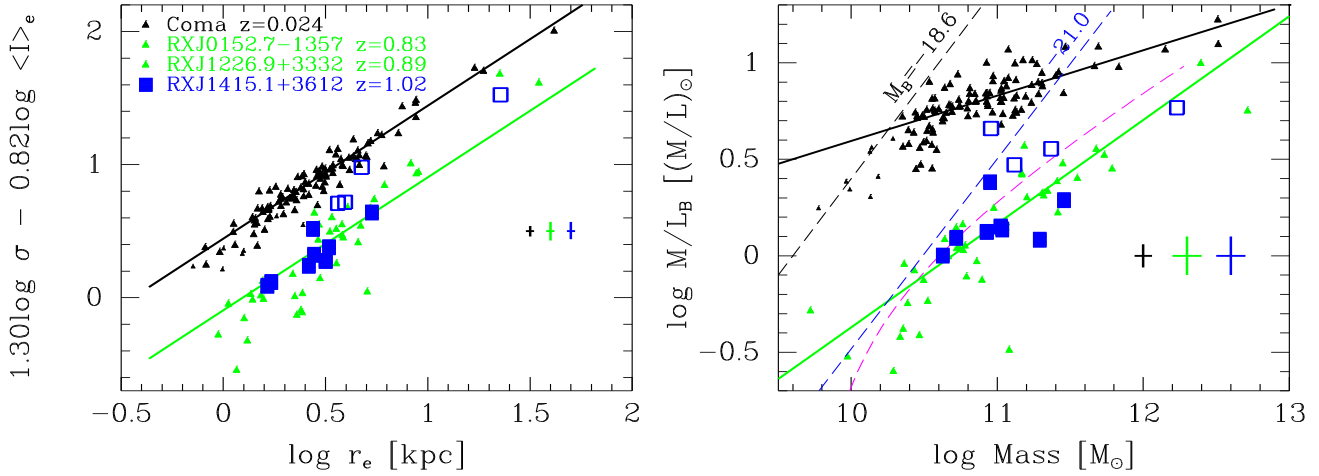


**Fig. 2** Fundamental Plane (FP) of early-type galaxies in RXJ0152.7-1357 ( $z = 0.83$ , green triangles), RXJ1226.9+3332 ( $z = 0.89$ , green triangles), both from Jørgensen et al. (2006, 2007), and RXJ1415.1+3612 ( $z = 1.02$ , blue squares). Left: Edge-on projection of FP. The Coma cluster is used as a local reference (black triangles, Jørgensen 1999). The solid black line represents the fit to the local Coma Cluster sample. The solid green line represents the fit to the Coma Cluster sample offset to the median zero-point of the two distant clusters at  $z = 0.8 - 0.9$ . Open symbols are galaxies with emission lines. Right:  $M/L - M$  plane. Dashed lines indicate the magnitude limits of Coma (black) and the distant cluster at  $z = 1$  (blue). Solid green line is the fit to the two clusters at  $z = 0.8 - 0.9$ . Internal uncertainties for the local reference, the two clusters at  $z = 0.8$  and the highest redshift cluster at  $z = 1$  are given as representative error bars. We find a mass-dependent evolution, where less massive galaxies show signatures of recent star formation episodes since  $z \sim 1.1 - 1.3$ . The dashed, magenta line shows the predictions of the single-burst stellar population models by Thomas et al. (2005).

of our surface brightness modelling using  $r^{1/4}$ -law profiles to model the luminosity distribution of our sample galaxies.

## 4 Results

### 4.1 A detailed FP of Cluster E+S0 galaxies at $z = 1$

As a first step we construct the FP for cluster E+S0 galaxies at  $z = 1$ . Fig. 2 shows the FP for the cluster E+S0 galaxies in the rest-frame Johnson  $B$ -band, compared to 116 early-type galaxies in the Coma cluster (Jørgensen 1999). The local reference is indicated with small triangles, whereas the distant E+S0 galaxies in RXJ1415.1+3612 at  $z = 1$  are displayed as the large squares. The two galaxy clusters RXJ0152.7-1357 and RXJ1226.9+3332 at  $z = 0.8 - 0.9$ , both from Jørgensen et al. (2006, 2007), are denoted as green triangles. Filled symbols denote E+S0 cluster members without emission lines, open symbols cluster galaxies with emission lines.

To limit differences in the sample selection of the Coma cluster and the high-redshift sample, low-mass galaxies with  $M < 10^{10.3} M_\odot$  as well as emission line galaxies were excluded. The FP of the Coma cluster (Jørgensen et al. 2006) is given by:

$$\log r_e = (1.30 \pm 0.08) \log \sigma - (0.82 \pm 0.03) \log \langle I_e \rangle + \gamma, \quad (1)$$

with  $\gamma = -0.443$ , denoted in Fig. 2 by the black solid line.

Fig. 2 presents the most detailed ever FP of cluster E+S0 galaxies at  $z = 1$ . The FP for galaxies at  $0.8 < z < 1.0$  has a different slope than the local Coma FP. The distant FP for

the high-redshift sample is not only offset from the local reference, but appears to have a steeper slope. The slope difference between the distant and the local relation is a strong indication of a mass-dependent evolution with a stronger evolution for less massive galaxies (see below). The results for the highest redshift cluster confirm previous findings for the two lower redshift clusters at  $z = 0.8 - 0.9$  by Jørgensen et al. (2006, 2007). Interestingly, RXJ1415.1+3612 cluster galaxies at  $z = 1$  with significant [O II] 3727 emission lines (defined with equivalent widths  $EW \geq -5 \text{ \AA}$ ; Balogh et al. 1997) are offset from the galaxies without emission lines and display a larger scatter. The galaxies with emission lines show higher  $M/L$  ratios than non-emission line galaxies, a trend which is opposite than expected. Partly this can be explained that the star formation in these galaxies is weak and that the net effect in the galaxy luminosity is small. Interestingly, also the Brightest Cluster Galaxy (BCG) exhibits weak star formation but follows the same FP relation as defined by the non-emission cluster members. In case of the BCG, the measured recent star formation activity could be explained with a ‘frosting’ scenario that does not move the galaxy away from the FP of the cluster galaxies at  $z = 1$ . The location of the other galaxies with emission lines is still an open question and will be investigated further in Jørgensen et al. (2009).

The observed evolution of the  $M/L$  ratio as derived from the FP depends on the age of the stellar population of the galaxies under consideration (e.g., Fritz et al. 2009). As the FP relation can be translated into a relationship between the  $M/L$  ratio and the stellar mass of a galaxy, an evolution

in the FP zero-point offset from the local FP relation with increasing redshift can be directly related to a change in the average  $M/L$  ratio of the galaxies (Djorgovski & Santiago 1993).

The distant cluster galaxies follow a steeper  $M/L$ -mass relation than the local reference (see Fig. 2). This slope change can be interpreted as a different dependence of the epoch of the most recent major star formation episode with the stellar mass of a galaxy. Less massive galaxies ( $M \sim 2 \times 10^{10} M_{\odot}$ ) have experienced their last major star formation burst at  $z_{\text{form}} \sim 1.1$ , whereas for massive galaxies ( $M > 2 \times 10^{11} M_{\odot}$ ) the majority of their stellar populations have been formed earlier  $z_{\text{form}} \gtrsim 1.6$ . Our results confirm previous findings by Jørgensen et al. (2006, 2007) for RXJ0152.7-1357 and RXJ1226.9+3332 at  $z = 0.8 - 0.9$ .

Using absorption-line strength data of nearby early-type galaxies in high-density environments, Thomas et al. (2005) predicted the SFHs of these galaxies for different galaxy masses. This single-burst stellar population (SSP) model is indicated as the dashed magenta line in Fig. 2. Both the relative timing of star formation ( $t_{\text{form}} < 11$  Gyr) and the slope change for less massive galaxies are consistent with our findings for the high-redshift clusters.

This result can be reconciled with the *down-sizing* formation scenario (Cowie et al. 1996). Massive galaxies are dominated by red old passively evolving stellar populations, whereas less massive systems have more extended SFH and continue to form stars at much later epochs. Both the mass assembly and SF are accelerated in massive systems in high density environments, whereas processes work on longer timescales in less massive (smaller) systems (Fritz 2007). Recent similar results derived for field E+S0 galaxies up to  $z \sim 1$  suggest that there is only a weak dependence of the overall galaxy properties with their environment (Fritz 2007; Fritz et al. 2009). The formation epoch of the field E+S0 galaxies depends mainly on their mass but only weakly on their luminosity, whereas the underlying environment regulates the time scales of the most recent star formation episodes. This gets support by similar results of a photometric study of cluster early-type galaxies at  $z = 1.24$  (Rettura et al. 2008).

## 5 Summary and Main Conclusions

Galaxies in clusters at intermediate redshift are useful probes to study the formation and the evolution of early-type galaxies. By measuring the kinematics and structure parameters of these galaxies their evolution in mass and mass-to-light ( $M/L$ ) ratios can be derived. This allows us to put constraints on the formation epoch and subsequent evolution of spheroidal galaxies up to the present-day as well as to critically test the models of galaxy formation and evolution.

In this paper we have presented the results of a detailed study of early-type galaxies in the distant clusters of galaxies RXJ1415.1+3612 at  $z = 1.013$ . Based on HST/ACS

imaging, surface brightness profiles, morphologies and structural parameters were derived for 30 galaxies within the HST/ACS field-of-view of the galaxy cluster. We have constructed the first detailed Fundamental Plane (FP) of 12 cluster early-type galaxies at redshift  $z = 1$ . This analysis is based on a sample size that represents a factor of 3 or more improvement compared to previous studies. We have combined our distant cluster sample with our previous detailed spectroscopic study of 38 early-type galaxies in two distant galaxy clusters at  $z = 0.8 - 0.9$ , RXJ0152.7-1357 and RXJ1226.9+3332 (Jørgensen et al. 2006, 2007). This allows us to study in more detail the early-type galaxy population in high redshift galaxy clusters up to redshift unity. Compared to the local reference, the distant cluster galaxies follow a steeper FP relation and  $M/L$ -mass relation. This slope change can be interpreted as a difference in the epoch of the last major star formation episode for galaxies with different stellar masses. The least massive galaxies ( $M = 2 \times 10^{10} M_{\odot}$ ) in our sample have experienced their most recent major star formation burst at  $z_{\text{form}} \sim 1.1$ , whereas for massive galaxies ( $M > 2 \times 10^{11} M_{\odot}$ ) the majority of their stellar populations have been formed earlier  $z_{\text{form}} \gtrsim 1.6$ . The dependence of the formation epoch on the mass confirms previous results by Jørgensen et al. (2006, 2007).

A similar mass-dependent evolution with more extended SFH has recently been found for field early-type galaxies (Fritz et al. 2009). Our results can be understood if less massive cluster galaxies have on average younger stellar populations. The distant galaxy population in these low-mass galaxies could have been built up over longer time scales and over more extended star formation histories of shorter duration but more frequent star formation bursts, compared to the formation history of the high-mass galaxy cluster counterparts.

Our results support a galaxy formation scenario according to the *down-sizing* picture (Cowie et al. 1996), where the mass of galaxies hosting star formation processes decreases with the age of the Universe. A combined analysis of the FP and the absorption line indices for RXJ1415.1+3612 as well as RXJ0152.7-1357 and RXJ1226.9+3332 will be presented in Jørgensen et al. (2009).

*Acknowledgements.* AF and IJ acknowledge support from grant HST-GO-10826.01 from STScI. STScI is operated by AURA, Inc., under NASA contract NAS 5-26555. Based on observations obtained at the Gemini Observatory under Gemini programs GN-2002B-SV-90, GN-2002B-Q-29, GN-2003A-SV-80, GN-2003A-DD-4, GN-2004A-Q-45, and GN-2005A-Q-33, which is operated by AURA, Inc., under cooperative agreement with the NSF, on behalf the Gemini Partnership: the NSF, STFC (UK), NRC (Canada), CONICYT (Chile), ARC (Australia), CNPq (Brazil), and SECYT (Argentina).

## References

- Bell, E. F. et al.: 2004, ApJ, 608, 752
- Balogh, M. L., et al.: 1997, ApJ, 488, L75

- Barr, J. et al.: 2005, AJ, 130, 445  
Barr, J. et al.: 2006, ApJ, 649, L1  
Bender, R., Burstein, D., & Faber, S. M. 1992, ApJ, 399, 462  
Bernardi, M. et al. 2003, AJ, 125, 1866  
Branchesi, M. et al.: 2006, A&A, 446, 97  
Carlstrom, J. E., Holder, G. P., Reese, E. D. 2002, ARA&A, 40, 643  
Chiboucas, K., Barr, J., Flint, K. et al.: 2009, ApJS, 184, 271  
Cooper, M. C., et al.: 2007, MNRAS, 376, 1445  
Cowie, L. L. et al.: 1996, AJ, 112, 839  
Cucciati, O., et al.: 2006, A&A, 458, 39  
Demarco, R., et al: 2007, ApJ, 663, 164  
di Serego Alighieri, S., et al.: 2005, A&A, 442, 125  
Djorgovski, S., & Davis, M.: 1987, ApJ, 313, 59  
Djorgovski, G., & Santiago, B. X.: 1993, in: I. J. Danzinger, W. W. Zeilinger, & K. Kjaer (eds.), *Structure, Dynamics and Chemical Evolution of Elliptical Galaxies*, p. 59  
Dressler, A., Lynden-Bell, D., Burstein, D., Davies, R. L., Faber, S. M., Terlevich, R., Wegner G.: 1987, ApJ, 313, 42  
Faber, S. M., et al.: 2007, ApJ, 665, 265  
Ferreiras, I. et al.: 2009, MNRAS, 396, 1573  
Finoguenov, A., et al.: 2007, ApJS, 172, 182  
Fritz, A. et al.: 2005, MNRAS, 358, 233  
Fritz, A.: 2007, PASP, 119, 590  
Fritz, A., Böhm, A., & Ziegler, B. L.: 2009, MNRAS, 393, 1467  
Gebhardt, K., Faber, S. M., Koo, D. C., et al.: 2003, ApJ, 597, 239  
Gladders, M. D., Yee, H. K. C.: 2005, ApJS, 157, 1  
Glazebrook, K., & Bland-Hawthorn, J.: 2001, PASP, 113, 197  
Holden, B. P. et al.: 2005, ApJ, 620, L83  
Hook, I. M. et al.: 2004, PASP, 116, 425  
Jørgensen, I., Franx, M., Kjaergaard, P. 1995, MNRAS, 273, 1097  
Jørgensen, I., Franx, M., & Kjaergaard, P.: 1996, MNRAS, 280, 167 (JFK96)  
Jørgensen, I.: 1999, MNRAS, 306, 607  
Jørgensen, I., Franx, M., Hjorth, J., & van Dokkum, P. G.: 1999, MNRAS, 308, 833  
Jørgensen, I., Bergmann, M., Davies, R., Jordi, B., Takamiya, M., & Crampton, D.: 2005, AJ, 129, 1249  
Jørgensen, I., Chiboucas, K., Flint, K., Bergmann, M., Barr, J., & Davies, R.: 2006, ApJ, 639, L9  
Jørgensen, I., Chiboucas, K., Flint, K., Bergmann, M., Barr, J., & Davies, R. 2007, ApJ, 654, L179  
Jørgensen, I., Fritz, A., Chiboucas, K., Schiavon, R. P., et al. 2009, AJ, in prep.  
Krist, J.: 1995, in: R. A. Shaw, H. E. Payne, & J. J. E. Hayes (eds.), *Astronomical Data Analysis Software and Systems IV*, ASPC 77, p. 349  
Lawrence, A., et al.: 2007, MNRAS, 379, 1599  
Lidman C., Rosati, P., Tanaka, M., et al.: 2008, A&A, 489, 981  
Mei, S., Holden B. P., Blakeslee J. P., et al.: 2009, ApJ, 690, 42  
Peng, C. Y., et al.: 2002, AJ, 124, 266  
Pozzetti, L., et al. 2009, A&A, submitted (arXiv:0907.5416)  
Rettura, A. et al.: 2008, ApJ, in press (arXiv:0806.4604)  
Romer, A. K., et al.: 2001, ApJ, 547, 594  
Rosati, P., Tozzi, P., Ettori, S. et al.: 2004, AJ, 127, 230  
Stanford, S. A., et al.: 2001, ApJ, 552, 504  
Stanford, S. A., et al.: 2005, ApJ, 634, L129  
Stanford, S. A., et al.: 2006, ApJ, 646, L13  
Thomas, D. et al.: 2005, ApJ, 621, 673  
Treu, T. et al.: 2005, ApJ, 633, 174  
van Dokkum, P. G., & Stanford, S. A.: 2003, ApJ, 585, 78  
Wuyts, S., van Dokkum, P. G., Kelson, D. D., Franx, M., & Illingworth, G. D.: 2004, ApJ, 605, 677